Impaired Apparent Ion Demand in Experimental Diabetic Retinopathy: Correction by Lipoic Acid

Bruce A. Berkowitz,[1,2] *Robin Roberts,*[1] *Ann Stemmler,*[3] *Hongmei Luan,*[1] *and Marius Gradianu*[1]

Purpose. To test the hypothesis that early in the course of diabetes, apparent ion demand within the retina is impaired and may be corrected by α-lipoic acid (LPA), a drug that inhibits vascular histopathology.

Methods. Intraretinal manganese ion uptake and retinal thickness were measured from high-resolution manganese-enhanced MRI (MEMRI) data of control and streptozocin diabetic male Sprague–Dawley (SD) rats and of control and diabetic female Lewis rats with and without treatment with LPA. In a subgroup of male SD rats, blood-retinal barrier (BRB) integrity was also assessed with dynamic contrast-enhanced MRI. In addition, ion-coupled plasma-mass spectrometry (ICP-MS) was used to measure baseline whole manganese levels from retinas of control and diabetic rats.

Results. Manganese ion uptake by receptor and postreceptor retina was subnormal in each untreated diabetic groups, and these deficiencies could be corrected with LPA treatment. ICP-MS studies found no differences in baseline retinal manganese concentration between control and diabetic rats. In 3-month-old diabetic male SD rats, total and postreceptor retinal thickness increased ($P < 0.05$) without loss of BRB integrity. In contrast, in untreated and treated diabetic female Lewis rats, retinal thicknesses were normal.

Conclusions. The present results support the hypothesis that LPA can correct the impaired apparent ion demand in experimental diabetic retinopathy. (*Invest Ophthalmol Vis Sci.* 2007; 48:4753–4758) DOI:10.1167/iovs.07-0433

Diabetic retinopathy is commonly considered a vascular disease and can be diagnosed and treated based on changes in the retinal circulation. Electroretinogram functional deficits of receptor (i.e., the combination of inner and outer segments of the photoreceptor, outer nuclear layer, and outer plexiform layer) and postreceptor (i.e., the combination of inner nuclear layer, inner plexiform layer, and ganglion cell layer) regions are documented before the appearance of vascular histopathology, but not before retinal vascular dysfunction.[1–3] Thus, a role for receptor and nonreceptor retina in diabetic retinopathy remains unclear.

Normal cellular activity supporting retinal function and healthy vision is strongly dependent on proper cellular demand for ions such as calcium. Hyperglycemia in experimental models is associated with perturbed levels of retinal ions (e.g., protons, sodium, magnesium, and calcium) and their regulatory systems.[4–7] Targets of diabetic complications, such as retina, nerve, heart, and liver, consistently demonstrate reduced activity of membrane-bound Na^+/K^+-ATPase, a member of P-type ATPases that are a large superfamily of ATP-driven pumps involved in the transmembrane transport of charged substrates.[6,8,9] Thus, measurement of demand for ions in vivo could provide useful information about cell activity associated with diabetic retinopathy.

We measure the initial uptake of manganese, after systemically administered $MnCl_2$, as a probe of ion demand related to cellular activity in different layers of the retina in vivo. Manganese ion (Mn^{2+}) is a surrogate for ions such as calcium,[10] an essential trace element,[11] and a strong MRI contrast agent.[10] In rats in vivo, high spatial resolution manganese-enhanced MRI (MEMRI) robustly measures manganese uptake in two dimensions, intraretinally (i.e., in different retinal layers) and panretinally (i.e., from each layer as it spans from ora serrata to ora serrata). We have previously shown that the MEMRI measurement of intraretinal manganese uptake is regulated by factors involved with ion usage, such as light/dark adaptation, sodium, potassium ATPase, and L-type calcium channels.[12–14] In addition, manganese influx into the retina is faster than its efflux.[14] Because we cannot discern whether changes in retinal manganese uptake result from alterations in transport or usage, we refer to intraretinal manganese uptake as a measure of apparent ion demand underlying cellular activity, and thus function, of each retinal layer. A goal of the present study was to determine whether apparent ion demand within the retina is a useful imaging biomarker of diabetic retinopathy (reflects early diabetes-induced changes within the retina, is predictive of treatment response, or both).

In this study, we used MEMRI to test the hypothesis that early in the course of diabetes, the apparent ion demand of receptor and postreceptor retina is impaired. To test whether any impairment of intraretinal uptake was a common defect linked with chronic hyperglycemia and not to a particular strain or sex or to diabetes duration, two combinations of different strains and sex of rats were examined in this study. In addition, we examined whether α-lipoic acid (LPA), a drug that prevents retinal vascular histopathology associated with diabetes, could correct the impairment of apparent ion demand within the retina.[15,16] LPA inhibits diabetes-induced reductions in ATPase activity in nerve and other tissues that develop complications, and we reasoned a similar effect may be found in the retina.[8,9,17] To the best of our knowledge, the impact of LPA treatment on diabetes-induced alternations of retinal ion demand has not been explored.

Methods

The animals used in our study were treated in accordance with the Principles of Laboratory Animal Care (NIH publication no. 85–23,

From the Departments of [1]Anatomy and Cell Biology, [2]Ophthalmology, and [3]Biochemistry and Molecular Biology, Wayne State University, Detroit, Michigan.

Supported by the National Institutes of Health (Grant EY010221 [BAB]), the Juvenile Diabetes Research Foundation (BAB), and Research to Prevent Blindness (grant to the Department of Ophthalmology).

Submitted for publication April 12, 2007; revised May 22 and June 25, 2007; accepted August 17, 2007.

Disclosure: **B.A. Berkowitz**, None; **R. Roberts**, None; **A. Stemmler**, None; **H. Luan**, None; **M. Gradianu**, None

The publication costs of this article were defrayed in part by page charge payment. This article must therefore be marked "*advertisement*" in accordance with 18 U.S.C. §1734 solely to indicate this fact.

Corresponding author: Bruce A. Berkowitz, Department of Anatomy and Cell Biology, Wayne State University School of Medicine, 540 E. Canfield, Detroit, MI 48201; baberko@med.wayne.edu.

revised 1985; http://grants1.nih.gov/grants/olaw/references/phspol.htm) and the ARVO Statement for the Use of Animals in Ophthalmic and Vision Research.

Groups

For the MRI studies, we studied age- and strain-matched controls (17 males, 12 females), 3-month-old diabetic male Sprague–Dawley (SD) rats ($n = 15$), and 4.5-month-old diabetic female Lewis rats ($n = 8$) fed either normal chow or chow-admixed LPA (400 mg/kg; $n = 8$). LPA chow was started 1 week after the induction of diabetes.

Diabetes was induced with intraperitoneal injection of streptozocin (60 mg/kg) within 5 minutes of its preparation in 0.01 M citrate buffer (pH 4.5) in rats with body weights of approximately 200 g after overnight fast. Diabetes was verified 3 days later by the presence of plasma hyperglycemia (≥300 mg/dL) and elevated urine volume (more than 60 mL/d) in nonfasted rats. Rat body weight and blood glucose levels were monitored weekly. Subtherapeutic levels of insulin (0–2 U neutral protamine Hagedorn insulin administered subcutaneously daily) were administered to maintain blood glucose levels between 450 and 550 mg/dL without urine ketones. Glycated hemoglobin was measured after 2 months of diabetes (Glyco-Tek affinity columns, kit 5351; Helena Laboratories, Beaumont, TX).

All rats were housed in normal 12-hour cycled laboratory lighting until the end of the experiment. Then they were maintained in darkness for 16 to 20 hours before manganese injection. All procedures (e.g., weighing, injecting $MnCl_2$, anesthetic administration, and MRI examination) were conducted under dim red light or darkness. $MnCl_2$ was administered as intraperitoneal injection (44 mg/kg) on the right side of awake rats. After this injection, rats were maintained in dark conditions for another 3.5 to 4 hours and were anesthetized for ICP-MS evaluation of retinal Mn^{2+} concentration or for retinal thickness and Mn^{2+} uptake measurements (MEMRI study). Note that postreceptor retinal thickness cannot be accurately assessed from the MEMRI images of dark-adapted rats because the similar manganese uptake in postreceptor and receptor retina reduces boundary contrast.[12] To determine postreceptor thickness, additional SD and Lewis control and diabetic rats were light adapted, as previously described, and then studied with MEMRI. In these light-adapted studies, apparent ion demand within the retina was not reported because the presence of a cataract in the diabetic rats (Fig. 1) caused the retinas to appear dark adapted on MEMRI examination, making comparisons with fully light-adapted control rats difficult (data not shown).

Inductively Coupled Plasma-Mass Spectrometry

We compared whole retinal manganese levels in age-matched controls (with and without $MnCl_2$ injection), 2-month-old diabetic female SD rats (no injection), and 3-month-old male SD rats (injection). An inductively coupled plasma–mass spectrometer (Sciex Elan 9000 ICP-MS; PerkinElmer, Waltham, MA) with a cross-flow nebulizer and Scott-type spray chamber was used for manganese concentration determination. The operating parameters of the spectrometer were optimized as follows: RF power, 1000 W; plasma gas flow, 15 L/min; nebulizer gas flow, 0.90 L/min. The optimum lens voltage was centered on rhodium sensitivity. Manganese was detected using the peak-hopping mode of the ICP-MS at m/z of 55 with a dwell time of 300 ms. To improve sensitivity, retinas of each rat were pooled, and the final weight was divided by 2. After overnight drying, 170 μL concentrated ultrapure nitric acid was added, followed by exposure to a heat block (80°C) for 2 hours with occasional vortexing. HPLC grade water was then added to each tube for a total known volume of 2.5 to 3 mL. Three standard solutions were used to generate a calibration curve (1, 5, and 25 ppb in manganese). Given that 1 ppb equals 1 μg/L and the total volume

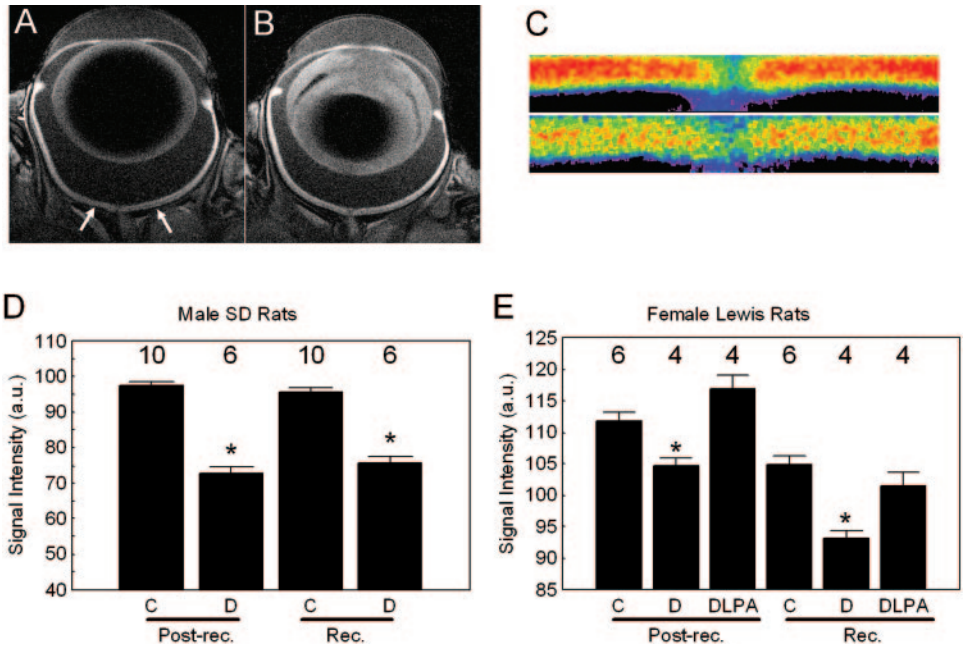

FIGURE 1. Representative high-resolution MEMRI data of (**A**) control and (**B**) 3-month-old diabetic male SD rats. *White arrows*: posterior region of the eye analyzed in this study. (**C**) Pseudocolor linearized images of average retinal signal intensity in the posterior retina of dark-adapted control male SD rats (*top*, $n = 10$) and diabetic male SD rats (*bottom*, $n = 6$). The same pseudocolor scale was used for both linearized images, where *blue* to *green* to *yellow* to *red* represent lowest to highest signal intensity. (**D**, **E**) Signal intensity data in postreceptor (Post-rec.) and receptor (Rec.) retina of control (C) and diabetic (D) groups examined in this study. (**E**) Data for the diabetic female Lewis rats treated with LPA (DLPA) are also shown. Note that the data for male and female groups were collected with different acquisition parameters and cannot be directly compared. Thus, percentage changes from control values were calculated and presented in the result. The numbers of animals used to generate these data are listed above each bar. Error bars represent the SEM. $^*P < 0.05$ was considered significant.

was known, the total amount of manganese (in micrograms) in the sample tubes (measured by ICP-MS) was divided by the dry weight to give the amount of manganese in micrograms per gram of dry retina.

MRI Data Acquisition

In all experiments, at the beginning of the MRI experiment, blood from the tail vein was collected and analyzed for glucose concentration. After the MRI examination, the anesthetized animals were humanely killed.

High-Resolution MRI

Immediately before the MRI experiment, rats were anesthetized using urethane (36% solution administered intraperitoneally, 0.083 mL/20 g animal weight, prepared fresh daily; Aldrich, Milwaukee, WI). Core temperatures were maintained using a recirculating heated water blanket. MRI data were acquired on a 4.7-T nuclear magnetic resonance system (Avance; Bruker, Billerica, CA) using a two-turn transmit/receive surface coil (1-cm diameter) placed over the eyes. A single transverse slice through the center of the eye (based on sagittal localizer images collected with the same adiabatic pulse sequence described) was obtained for each rat. Transverse images were then acquired using an adiabatic spin-echo imaging sequence (repetition time, 350 seconds; echo time, 16.7 ms; number of acquisitions, 16; sweep width, 61,728 Hz; matrix size, 256 × 512 [Lewis rats] or 512 × 512 [SD rats]; slice thickness, 620 μm; field of view, 12 × 12 mm^2).[18]

Blood-Retinal Barrier Integrity

Measurement of blood-retinal barrier (BRB) integrity was assessed as described previously.[19] Briefly, urethane-anesthetized rats had their tail veins cannulated with a 25-g catheter and were then gently positioned on an MRI-compatible holder. An adiabatic spin-echo imaging sequence was used with the following parameters: repetition time, 1 second; echo time, 22.7 ms; number of acquisitions, 1; matrix size, 128 × 256; slice thickness, 1 mm; field of view, 32 × 32 mm^2; sweep width, 25,000 Hz; 2 minutes/image. Twelve sequential 2-minute images were acquired as follows: three control images before injection of contrast agent and nine images during and after a 6-second Gd-DTPA bolus injection. The dose of contrast agent (Gd-DTPA, Magnevist; Berlex Laboratories, Wayne, NJ) was 0.1 mM/L/kg. In each animal, Gd-DTPA was injected at the same phase-encode step collected near the beginning of the fourth image.

Data Analysis

Retinal Thickness. Total (light and dark adapted) and postreceptor (light adapted only) retinal thicknesses were manually measured from superior and inferior retinas at six different locations per side as the radial distance between the anterior and posterior edges of the retina or anterior and border of postreceptor and receptor retina, respectively, 0.4 to 1 mm from the optic nerve. No differences between superior and inferior hemiretinal thickness values were noted (data not shown). Thus, averaged data were used for comparisons.

Layer-Specific Signal Intensity. For visualization and comparison purposes, in-house written software was used to map the in situ image into a linear representation for each retina. Within each group, linearized retinas were averaged into a composite image. For quantitative analysis, signal intensities were analyzed using the program IMAGE (a freeware program available at http://rsb.info.nih.gov/nih-image) and derived macros.[20] Changes in receiver gain between animals were controlled for by setting the signal intensity of a fixed region of noise in each rat to a fixed value. Other tissues within the sensitive volume of the coil demonstrated enhancement after manganese injection and were considered inadequate as internal references. Postreceptor and receptor signal intensity data (from the edge of the optic nerve to 1 mm from the center of the optic nerve) were extracted. The border between postreceptor and receptor retina was set at 4 pixels posterior to the clearly defined vitreoretinal division. We then drew another border between the retina and the choroid 3 pixels posterior from postreceptor/receptor division (i.e., receptor division). Pixels immediately anterior to these borders were considered representative of postreceptor and receptor retina, respectively, and were analyzed as described.

Passive Blood-Retinal Barrier Permeability Surface Area Product/Gd-DTPA. BRB permeability surface area product (BRB PS) was estimated as previously described.[21] Briefly, after coregistration, the MRI data were analyzed using NIH IMAGE. The three precontrast images were averaged to improve the signal-to-noise ratio. For each pixel, the fractional signal enhancement, E, was calculated as described.[21] A region of interest (ROI) was chosen on the E map that contained the entire vitreous space. The area of this ROI and the mean E within the ROI were measured at each postcontrast time point. Only the last four time points (13, 15, 17, and 19 minutes) were converted to BRB PS values.[21] These PS values were then averaged to minimize the influence of noise on any one PS value.

Statistical Analysis

Retinal thickness and permeability data were consistent with a normal distribution, and comparisons between groups were performed using an unpaired 2-tailed *t*-test analysis. Comparisons of MEMRI retinal signal intensities were performed using a generalized estimating equation (GEE) approach.[12,22] GEE performs a general linear regression analysis using all the pixels in each subject and accounts for the within-subject correlation between adjacent pixels. In all cases, $P \leq 0.05$ was considered statistically significant. Data are presented as mean ± SEM unless otherwise noted.

Results

Systemic Physiology

Summaries of group body weights and glycated hemoglobins are presented in Table 1.

MEMRI

Representative high-resolution images for control (Fig. 1A) and diabetic male SD rats (Fig. 1B) are presented. The extent of cataract in diabetic rats could be readily visualized (Fig. 1B). In all groups, signal enhancements consistent with the retention of Mn^{2+} were evident within postreceptor and receptor retina of control and diabetic rats (Figs. 1C–E).Visual inspection of mean linearized images about the optic nerve suggested that in diabetic rats apparent ion demand within the retina is lower than in controls (Fig. 1C).

Male SD Rats

Diabetes reduced apparent ion demand from control values in postreceptor retina by 24.6% ± 1.8% ($P < 0.05$) and in receptor retina by 19.8% ± 1.7% ($P < 0.05$).

Table 1. Summary of Body Weights and Glycated Hemoglobins

Group	Body Weight (g)	Glycated Hemoglobin (%)
Control male SD	490.4 ± 7.6	5.4 ± 0.2
Diabetic male SD	370.8 ± 6.5*	13.0 ± 0.3*
Control female Lewis	264.0 ± 3.1	4.5 ± 0.1
Diabetic female Lewis	228.6 ± 3.6*	11.4 ± 0.3*
Diabetic + LPA female Lewis	234.1 ± 4.1*	11.0 ± 0.6*

Values are expressed as mean ± SEM.
* $P < 0.05$ compared with respective control values.

Female Lewis Rats

Compared with control values, chronic hyperglycemia lowered apparent ion demand by 6.5% ± 1.1% ($P < 0.05$) in postreceptor retina and 11.2% ± 1.2% ($P < 0.05$) in receptor retina. The change in apparent ion demand within the retina from the respective mean control value for the diabetic female Lewis group was relatively lower ($P \leq 0.05$) than that for the diabetic male. Preventive LPA treatment corrected these deficits throughout the retina ($P < 0.05$; Fig. 1E).

Retinal Thickness

Male SD Rats. Quantitative analysis revealed that diabetic male SD rats had a total retinal thickness (227.2 ± 1.3 μm; $n = 15$) greater than that of controls (204.9 ± 1.5 μm; $n = 17$; $P < 0.05$; Fig. 2). Postreceptor retinal thickness (104.0 ± 0.5 μm; $n = 7$) was also greater than that in controls (97.9 ± 1.3 μm; $n = 7$; $P < 0.05$). BRB PS in diabetic rats ($2.4 \pm 0.8 \times 10^{-6}$ cm^3/min; $n = 5$) was not different ($P > 0.05$) from that in control rats ($2.9 \pm 0.3 \times 10^{-6}$ cm^3/min; $n = 6$).

Female Lewis Rats. In untreated diabetic female Lewis rats, total (221.4 ± 4.7 μm; $n = 8$) and postreceptor (101.9 ± 6.9 μm; $n = 3$) retinal thicknesses were not different ($P < 0.05$) from those in controls (218.2 ± 2.3 μm [$n = 12$] and 93.0 ± 2.4 μm [$n = 4$], respectively) or in LPA-treated diabetic female Lewis rats (216.0 ± 5.3 μm [$n = 8$] and 96.3 ± 3.9 μm [$n = 3$]; Fig. 2). Total retinal thicknesses of control male SD (204.9 ± 1.5 μm) and female Lewis rats (218.2 ± 2.3 μm) were also different ($P < 0.05$). BRB integrity was not examined in female Lewis rats because their retinal thicknesses were normal.

ICP-MS Retinal [Mn^{2+}]. In control rats, no difference ($P > 0.05$) in baseline retinal manganese concentrations was found between control rats (0.70 ± 0.1 μg/g dry retina; $n = 4$) and 2-month-old diabetic rats (0.9 ± 0.2 μg/g dry retina; $n = 4$). Preliminary efforts to use ICP-MS to measure whole retinal manganese levels after $MnCl_2$ injection intraperitoneally in control and diabetic male SD rats could not detect subtle differences between these groups because of the large variability in the estimate (data not shown).

Discussion

The major results of this study are that: (1) regardless of the combinations of strain and sex of rats examined, chronic hyperglycemia produced a subnormal uptake of manganese in photoreceptor and postreceptor retina before the reported appearance of vascular histopathology[23]; (2) diabetic male SD rats demonstrated relatively more severe impairment in manganese uptake and supernormal retinal thickness than diabetic female Lewis rats; (3) preventive LPA treatment, at a dose and a route reported to minimize diabetes-related retinal vascular histopathology, corrected apparent ion demand deficiencies within the retina; and (4) strain/sex differences in retinal thickness at baseline and in response to diabetes appear to be independent of changes in BRB permeability. These results highlight, for the first time, apparent ion demand as a useful imaging biomarker for early monitoring of diabetic retinopathy and its treatment response, and they underscore that MEMRI is a powerful approach for robustly and simultaneously studying changes in intraretinal activity and retinal thickness in vivo.[12]

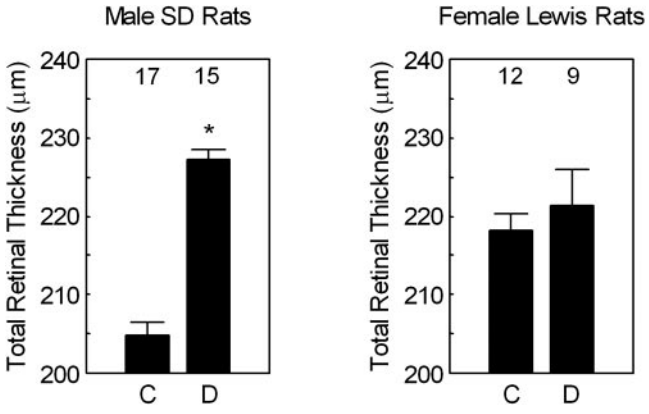

Figure 2. Total retinal thickness measurements are presented for control (C) and diabetic (D) rats in the male SD (*left*) and female Lewis (*right*) groups. The numbers of animals used to generate these data are listed above each bar. Error bars represent the SEM. *$P < 0.05$ was considered significant.

The mechanisms responsible for diabetes-induced reduction in intraretinal manganese uptake are unknown. One possibility is that diabetes increased baseline retinal manganese levels with the result that less manganese is taken up.[6,7,24] However, through the use of ICP-MS, we found no evidence for increased baseline levels of retinal manganese between control and diabetic groups. Another possibility is that diabetic rats had lower levels of manganese in their plasma after systemic injection. Although we did not measure plasma manganese levels in this study, it is unclear how, if all groups received the same systemic dose of $MnCl_2$, diabetes could reduce plasma manganese levels. We also note that in a preliminary study in control female SD rats, systemic injection of 15 mg/kg $MnCl_2$ did not result in a decrease ($P > 0.05$) in intraretinal signal intensity 4 hours after injection compared with that measured after injection of 44 mg/kg $MnCl_2$ (data not shown). A third possibility is that the decrease in apparent ion demand could have resulted from manganese toxicity. Using the same dose of manganese as in this present study, no alterations in inner or outer electroretinographic parameters were found 4 hours and 7 days after injection.[14] In addition, no changes were measured in retinal thickness or increased BRB leakage 1 month after administration.[12] Thus, the present dose and route of the manganese are considered nontoxic.

A fourth possibility is that reduced retinal manganese uptake reflected a decrease in apparent ion demand within the retina associated with chronic hyperglycemia. Diabetes reduces the activity of major regulators of ion homeostasis (e.g., Na^+/K^+-ATPase, calcium ATPase, and ion exchangers) in retina and in other tissues that develop complications, perhaps by increasing lipid peroxidation and protein glycation.[4,6,8,9,25,26] These ATPases and exchangers, working individually and together, maintain healthy vision by modulating cation gradients during dark current generation in the photoreceptors, synaptic activity throughout the retina, action potentials in ganglion cells, and neurotransmitter uptake by Müller cells, and they help protect the retina from cytotoxic edema (i.e., edema that forms in the presence of an intact BRB).[6,27–31] Previously, we found that treatment with intravitreal ouabain, at a dose that inhibited retinal Na^+/K^+-ATPase activity, resulted in subnormal intraretinal manganese uptake.[14,29,32] One explanation for this subnormal manganese uptake is that ouabain-induced reduction in Na^+/K^+-ATPase activity increases intracellular sodium levels, which, in turn, inhibits Na^+/Ca^{2+}exchanger activity, and, we speculate, manganese uptake.[25] We note that ouabain-induced reduction in manganese uptake (19.8%–23.9%) is intriguingly similar to that measured in this study for diabetic male SD rats (19.8%–24.6%).[14] These considerations are consistent with our premise that reduced intraretinal uptake of Mn^{2+} in diabetic rats was partly caused by diabetes-induced reduction in ion demand.

The major goal of this study was to compare intraretinal manganese uptake in different strains, sex, and diabetes dura-

tion to determine whether subnormal uptake is a common defect linked with chronic hyperglycemia. Incidentally, we observed an unexpected differential change in retinal thickness after 3 to 4.5 months of diabetes in male SD rats but not female Lewis rats. There has been little consistency in retinal thickness, measured ex vivo, as a function of diabetes in different laboratories. For example, retinal thinning was found on histology after several months of diabetes in male SD rats, asymmetrical retinal thinning was measured on MRI after 3 months of diabetes in female SD rats, and temporarily increased retinal thickness was reported from histology in diabetic male SD rats.[33–35] In addition, in diabetic rodents, BRB is reported to be intact or increased.[19] We speculate that such interlaboratory variability in retinal thickness and BRB integrity measurements at least partly results from examination of these parameters in separate groups of animals using ex vivo techniques which may be confounded by death and processing artifacts.[19] The present data support the use of MEMRI to accurately monitor retinal thickness and BRB data in the same rat in vivo.[12,19,33] However, more work is clearly needed to examine the strain/sex/diabetes duration differences reported in this study before identifying the important factors linked with the differential retinal thickness between groups.[36,37]

In this study, we found that in female Lewis rats, the diabetes-related decreased apparent ion demand within the retina could be corrected using LPA treatment. The results of this study do not rule out the possibility that LPA is effective only in Lewis rats. However, this prospect appears unlikely because LPA has demonstrated effective oxidative stress reduction in the retinas of diabetic SD rats. In addition, several groups, using diabetic Wistar rats, found that LPA treatment reduces the level of oxidative stress, normalizes NF-κB activation and angiopoietin-2 expression, reduces vascular endothelial growth factor, and inhibits acellular capillaries and pericyte ghosts.[15,16,38,39] LPA has also been reported to correct diabetes-induced abnormalities in retinal ΔPo_2, a prognostic biomarker of treatment efficacy, and to inhibit the appearance of acellular capillaries and pericyte ghosts in a rat STZ model.[8,9,15,16,40,41] LPA can lower lipid peroxidation and protein glycosylation and can increase ATPase activities.[8,9,15–17,40] Ouabain inhibition of sodium-potassium ATPase in control rats produces a subnormal retinal uptake of manganese.[14] Thus, we speculate that correcting factors that affect ATPase activity, such as disruption of lipid membranes through diabetes-induced lipid peroxidation and protein glycosylation with the use of LPA may be the mechanism by which diabetes-induced subnormal uptake of manganese is prevented. A correctional effect of LPA on BRB integrity was not investigated because BRB permeability was not increased in any group in this study. The current data raise the possibility of an important link between diabetes, subnormal retinal ion demand, and subsequent vascular pathophysiology and histopathology findings.

Acknowledgments

We thank Tim Kern for helpful discussions and review of this manuscript.

References

1. Phipps JA, Fletcher EL, Vingrys AJ. Paired-flash identification of rod and cone dysfunction in the diabetic rat. *Invest Ophthalmol Vis Sci*. 2004;45(12):4592–4600.
2. Barber AJ. A new view of diabetic retinopathy: a neurodegenerative disease of the eye. *Prog Neuropsychopharmacol Biol Psychiatry*. 2003;27(2):283–290.
3. Trick GL, Berkowitz BA. Retinal oxygenation response and retinopathy. *Prog Retin Eye Res*. 2005;24(2):259–274.
4. Cukiernik M, Hileeto D, Downey D, et al. The role of the sodium hydrogen exchanger-1 in mediating diabetes-induced changes in the retina. *Diabetes Metab Res Rev*. 2004;20(1):61–71.
5. Ng YK, Zeng XX, Ling EA. Expression of glutamate receptors and calcium-binding proteins in the retina of streptozotocin-induced diabetic rats. *Brain Res*. 2004;1018(1):66–72.
6. MacGregor LC, Matschinsky FM. Altered retinal metabolism in diabetes, II: measurement of sodium-potassium ATPase and total sodium and potassium in individual retinal layers. *J Biol Chem*. 1986;261(9):4052–4058.
7. Budzynski E, Wangsa-Wirawan N, Padnick-Silver L, Hatchell D, Linsenmeier R. Intraretinal pH in diabetic cats. *Curr Eye Res*. 2005;30:229–240.
8. Stevens MJ, Obrosova I, Cao X, Van Huysen C, Greene DA. Effects of DL-alpha-lipoic acid on peripheral nerve conduction, blood flow, energy metabolism, and oxidative stress in experimental diabetic neuropathy. *Diabetes*. 2000;49(6):1006–1015.
9. Jain SK, Lim G. Lipoic acid decreases lipid peroxidation and protein glycosylation and increases (Na(+) + K(+))- and Ca(++)-ATPase activities in high glucose-treated human erythrocytes. *Free Radic Biol Med*. 2000;29(11):1122–1128.
10. Lin YJ, Koretsky AP. Manganese ion enhances T1-weighted MRI during brain activation: an approach to direct imaging of brain function. *Magn Reson Med*. 1997;38(3):378–388.
11. Gong H, Amemiya T. Ultrastructure of retina of manganese-deficient rats. *Invest Ophthalmol Vis Sci*. 1996;37(10):1967–1974.
12. Berkowitz BA, Roberts R, Goebel DJ, Luan H. Noninvasive and simultaneous imaging of layer-specific retinal functional adaptation by manganese-enhanced MRI. *Invest Ophthalmol Visl Sci*. 2006;47(6):2668–2674.
13. Berkowitz BA, Roberts R, Penn JS, Gradianu M. High-resolution manganese-enhanced MRI of experimental retinopathy of prematurity. *Invest Ophthalmol Vis Sci*. 2007;48(10):4733–4740.
14. Berkowitz BA, Roberts R, Luan H, et al. Manganese-enhanced MRI studies of alterations of intraretinal ion demand in models of ocular injury. *Invest Ophthalmol Vis Sci*. 2007;48(8):3796–3804.
15. Kowluru RA, Odenbach S. Effect of long-term administration of alpha-lipoic acid on retinal capillary cell death and the development of retinopathy in diabetic rats. *Diabetes*. 2004;53(12):3233–3238.
16. Lin J, Bierhaus A, Bugert P, et al. Effect of R-(+)-alpha-lipoic acid on experimental diabetic retinopathy. *Diabetologia*. 2006;49:1089–1096.
17. Arivazhagan P, Panneerselvam C. Alpha-lipoic acid increases Na+K+ATPase activity and reduces lipofuscin accumulation in discrete brain regions of aged rats. *Ann NY Acad Sci*. 2004;1019:350–354.
18. Schupp DG, Merkle H, Ellermann JM, Ke Y, Garwood M. Localized detection of glioma glycolysis using edited 1H MRS. *Magn Reson Med*. 1993;30(1):18–27.
19. Berkowitz BA, Roberts R, Luan H, Peysakhov J, Mao X, Thomas KA. Dynamic contrast-enhanced MRI measurements of passive permeability through blood retinal barrier in diabetic rats. *Invest Ophthalmol Vis Sci*. 2004;45(7):2391–2398.
20. Berkowitz BA. Adult and newborn rat inner retinal oxygenation during carbogen and 100% oxygen breathing: comparison using magnetic resonance imaging delta PO_2 mapping. *Invest Ophthalmol Vis Sci*. 1996;37(10):2089–2098.
21. Berkowitz BA, Tofts PS, Sen HA, Ando N, de Juan E Jr. Accurate and precise measurement of blood-retinal barrier breakdown using dynamic Gd-DTPA MRI. *Invest Ophthalmol Vis Sci*. 1992;33(13):3500–3506.
22. Liang Z. Longitudinal data analysis using generalized linear models. *Biometrika*. 1986 1;73:13–22.
23. Berkowitz BA, Ito Y, Kern TS, McDonald C, Hawkins R. Correction of early subnormal superior hemiretinal ΔPO_2 predicts therapeutic efficacy in experimental diabetic retinopathy. *Invest Ophthalmol Vis Sci*. 2001;42(12):2964–2969.
24. Szabo ME, Haines D, Garay E, et al. Antioxidant properties of calcium dobesilate in ischemic/reperfused diabetic rat retina. *Eur J Pharmacol*. 2001;428(2):277–286.

25. Moore ED, Etter EF, Philipson KD, et al. Coupling of the $Na^{+}/Ca2^{+}$ exchanger, Na^{+}/K^{+} pump and sarcoplasmic reticulum in smooth muscle. *Nature*. 1993;365(6447):657–660.
26. Cai X, Lytton J. The cation/Ca(2+) exchanger superfamily: phylogenetic analysis and structural implications. *Mol Biol Evol*. 2004; 21(9):1692–1703.
27. Winkler BS. Relative inhibitory effects of ATP depletion, ouabain and calcium on retinal photoreceptors. *Exp Eye Res*. 1983;36(4):581–594.
28. Malek SA, Adorante JS, Stys PK. Differential effects of Na-K-ATPase pump inhibition, chemical anoxia, and glycolytic blockade on membrane potential of rat optic nerve. *Brain Res*. 2005;1037(1–2):171–179.
29. Blanco G, Mercer RW. Isozymes of the Na-K-ATPase: heterogeneity in structure, diversity in function. *Am J Physiol*.1998;275(5 pt 2):F633–F650.
30. Fraser CL, Kucharczyk J, Arieff AI, Rollin C, Sarnacki P, Norman D. Sex differences result in increased morbidity from hyponatremia in female rats. *Am J Physiol*. 1989;256(4 pt 2):R880–R885.
31. Ames A III, Li YY, Heher EC, Kimble CR. Energy metabolism of rabbit retina as related to function: high cost of Na^{+} transport. *J Neurosci*. 1992;12(3):840–853.
32. Yuan Z, Cai T, Tian J, Ivanov AV, Giovannucci DR, Xie Z. Na/K-ATPase tethers phospholipase C and IP3 receptor into a calcium-regulatory complex. *Mol Biol Cell*. 2005;16(9):4034–4045.
33. Luan H, Roberts R, Sniegowski M, Goebel DJ, Berkowitz BA. Retinal thickness and subnormal retinal oxygenation response in experimental diabetic retinopathy. *Invest Ophthalmol Vis Sci*. 2006;47(1):320–328.
34. Park SH, Park JW, Park SJ, et al. Apoptotic death of photoreceptors in the streptozotocin-induced diabetic rat retina. *Diabetologia*. 2003;46(9):1260–1268.
35. Barber AJ, Lieth E, Khin SA, Antonetti DA, Buchanan AG, Gardner TW. Neural apoptosis in the retina during experimental and human diabetes: early onset and effect of insulin. *J Clin Invest*. 1998;102(4):783–791.
36. Ramsey DJ, Ripps H, Qian H. An electrophysiological study of retinal function in the diabetic female rat. *Invest Ophthalmol Vis Sci*. 2006;47(11):5116–5124.
37. Salyer DL, Lund TD, Fleming DE, Lephart ED, Horvath TL. Sexual dimorphism and aromatase in the rat retina. *Brain Res Dev Brain Res*. 2001;31126(1):131–136.
38. Obrosova IG, Fathallah L, Greene DA. Early changes in lipid peroxidation and antioxidative defense in diabetic rat retina: effect of DL-alpha-lipoic acid. *Eur J Pharmacol*. 2000;398(1):139–146.
39. Dene BA, Maritim AC, Sanders RA, Watkins JB III. Effects of antioxidant treatment on normal and diabetic rat retinal enzyme activities. *J Ocul Pharmacol Ther*. 2005;21(1):28–35.
40. Obrosova IG, Minchenko AG, Marinescu V, et al. Antioxidants attenuate early up regulation of retinal vascular endothelial growth factor in streptozotocin-diabetic rats. *Diabetologia*. 2001;44(9): 1102–1110.
41. Roberts R, Luan H, Berkowitz BA. α-Lipoic acid corrects late-phase supernormal retinal oxygenation response in experimental diabetic retinopathy. *Invest Ophthalmol Vis Sci*. 2006;47(9):4077–4082.